Canadian Conference - Pacific Conference on Earthquake Engineering 2023
Vancouver, British Columbia
June 25th – June 30th, 2023

Site-Specific Seismic Source Model and Acceleration Response Spectra for Stiff Soil Sites, Port Moresby, Papua New Guinea

Emma Watson[1], Erin Todd[2] and Alan Hull[3*]

[1]Engineering Seismologist/Geologist, WSP New Zealand, Christchurch, New Zealand
[2]Senior Engineering Seismologist, WSP New Zealand, Christchurch, New Zealand
[3]Senior Vice President, WSP USA Inc., Portland, Oregon, USA
[*]alan.hull@wsp.com (Corresponding Author)

ABSTRACT

We present a seismic source model for Port Moresby, Papua New Guinea based on modifying source zones developed for the 2016 and 2019 National Seismic Hazard Model (NSHM) for Papua New Guinea. We modified earlier seismic source models by combining area source zones, recalculating earthquake activity rate parameters for nine uniform-area source zones, redefining subduction zone interface sources, applying the 2020 NGA-Sub ground motion models (GMM), and segmenting the Owen Stanley fault source.

We used OpenQuake v.3.11 to calculate mean spectral accelerations from peak ground acceleration (PGA) to 10 s. Hazard calculations assume a site ground condition with a time-averaged shear-wave velocity in the 30 m below ground surface (V_{S30}) of 760 m/s. Acceleration calculations use four equally weighted crustal Next Generation Attenuation Relationships (NGA-West2) GMMs for crustal sources, and three equally weighted NGA-Sub GMMs for the subduction zone interface and in-slab sources. The 1/475 and 1/2,475 AEPs mean PGAs are 0.30 g and 0.53 g, respectively. Shallow crustal earthquakes (Mw 5.75 to Mw 6.5) at distances less than about 40 km dominate the 1/2,475-AEP hazard at periods less than 1.0 s for Port Moresby. At distances less than about 100 km, Mw 7+ earthquakes dominate the hazard at periods longer than about 1.0 s.

The revised source model has a mean 1/2,475 AEP PGA about double the 2019 NSHM value. Differences between this assessment and the 2019 NSHM decrease with increasing period and are similar for periods longer than about 2 s. Different source modelling models and GMMs used in the two studies are the main source of the differences in hazard, particularly the used of uniform-area rather than gridded-area for background earthquake source zones.

Keywords: Port Moresby, seismic source model, acceleration response spectra, hazard curves, Owen Stanley fault

INTRODUCTION

A recent increase in investment into Papua New Guinea (PNG) has led to increased demand for larger and taller buildings in the PNG capital city of Port Moresby. Because the PNG building code is based on scientific understandings more than 40 years old, some developers wish to apply international standards such as the American Society of Civil Engineers (ASCE) 7-16 and 7-22 and Eurocode 8 in Port Moresby. There is, therefore, a need for up-to-date seismic parameters to support structural design while the PNG building code update is in progress.

Some of the need for updated seismic parameters is met by a 2019 National Seismic Hazard model (NSHM) developed by Geoscience Australia for all of PNG. Unfortunately, this model does not provide discrete ground acceleration values for Port Moresby, so any seismic parameters must be interpolated from small-scale maps. Our motivation for this assessment is, therefore, to provide seismic parameters for stiff-soil sites in Port Moresby to assist in ongoing and planned developments. Our model offers one approach that can inform the development of a revised NSHM and in-progress update of the PNG building code.

SEISMIC SOURCE MODEL

We constructed a seismic source model to estimate earthquake ground motions in Port Moresby that reflects the present understanding of the local and regional geology, regional seismotectonics, and the spatial distribution of recorded earthquakes within the wider PNG region. The model incorporates known earthquake sources including plate boundary subduction zones (interface and in-slab sources), crustal faults, and background seismicity (i.e., earthquakes not associated with known, surface-rupturing faults or other known discrete sources). This information is used to define seismic source zones and quantify their rates and magnitudes of earthquakes as the basis to calculate the probabilistic hazard for Port Moresby.

Seismotectonic Setting

Papua New Guinea is part of the northern margin of the Australian tectonic plate (Figure 1). The tectonic complexity of the region results from the interactions between the Pacific and Caroline Sea tectonic plates as they obliquely converge with the Australian plate to the south (e.g., [1], [2], [3]). This boundary zone between the Australian, Pacific, and Caroline Sea plates comprises a series of seismically active subduction zones, small microplates with different rates and directions of movement, and major crustal faults that accommodate complex plate boundary deformations. This ongoing deformation generates many earthquakes including several large-magnitude (e.g., moment magnitude [Mw] 7 and greater) historical earthquakes.

The Pacific plate obliquely converges with the Australian plate at approximately 110 mm/yr (Australia fixed) in the west-southwest direction [2]. Northeast of Port Moresby, plate convergence results in present-day subduction of the Solomon Sea microplate beneath the Pacific plate along the New Britain Trench. In addition, subduction occurs along the boundaries of microplates located to the north and east of Papua New Guinea, such as the North Bismarck plate and possibly the Woodlark plate. The New Guinea Highlands are bounded along their southwest margin by the northeast-dipping Southern Highlands Thrust fault. The major Owen Stanley fault to the north of Port Moresby extends along the Papuan Peninsula and separates the Woodlark microplate to the north and the Australian plate to the south (Figure 1).

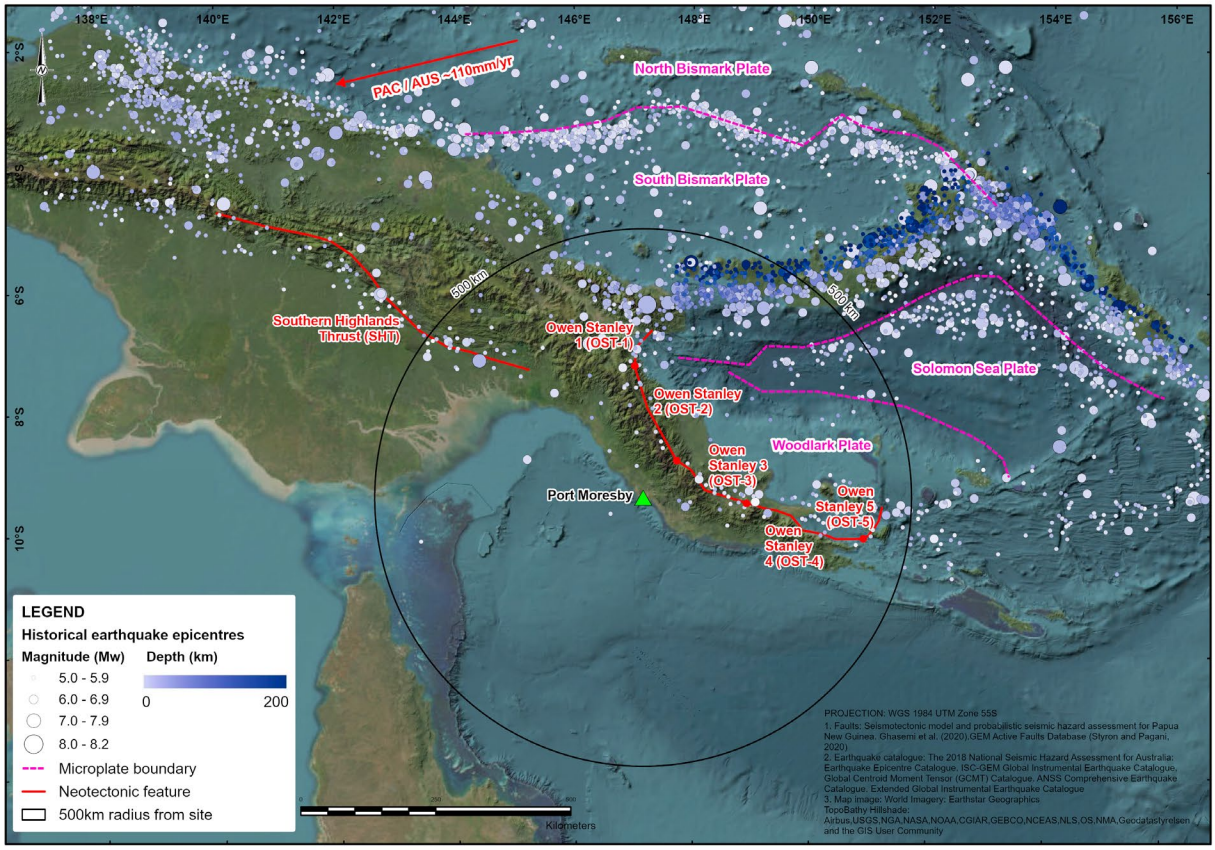

Figure 1: Seismotectonic setting of Port Moresby.

Earthquake Catalogs

We compiled an earthquake catalog for seismic source modelling from the following regional and global catalogs (listed in order of preference) for earthquakes of Mw greater than 3.0:

- The 2018 National Seismic Hazard Assessment for Australia: Earthquake Epicentre Catalog; regional catalogue (https://www.ga.gov.au/about/projects/safety/nsha, GA 2021). [4]
- ISC-GEM Global Instrumental Earthquake Catalog; global catalog (http://www.isc.ac.uk/iscgem/request_catalog.php, Version 8.0, ISC 2021). [5]
- Global Centroid Moment Tensor (GCMT) Catalog; global catalog [6]; http://www.globalcmt.org/CMTsearch.html.
- ANSS Comprehensive Earthquake Catalog; global catalog (https://earthquake.usgs.gov/earthquakes/search, [7]).
- Extended Global Instrumental Earthquake Catalog; global catalog [8].

The catalogs were combined, duplicate events removed through automatic and manual procedures, and earthquake magnitudes converted to the Mw scale for analytical consistency. The relations of [5] were used to convert between surface-wave magnitude (M_S) and Mw, and body-wave magnitude (mb) and Mw for the ISC-GEM catalog. Other magnitude measures were treated as equivalent to Mw. A spatiotemporal filter was applied to the combined catalog to detect duplicate earthquakes between catalogs within a prescribed time and spatial window. In general, the size of the time and spatial windows increases backwards in time to account for the lower resolution of older earthquake locations and origin times. For example, duplicate earthquakes pre-1900 were removed if they fell within 500 km and/or ±24 hours of each other. All earthquakes in the catalog with Mw >6.0 were manually checked to ensure duplicates were correctly removed.

The combined, uniform-magnitude earthquake catalog was declustered using the method of [9], then evaluated for temporal completeness. The procedures of [10] were applied to the declustered project catalog to evaluate completeness. The cumulative number of earthquakes was evaluated for various time and magnitude intervals to validate catalog completeness.

Source Modelling Approach

The seismotectonic model was developed from the available published geological, tectonic, and seismological information. A seismic source model is defined in terms of parameters such as source location, source geometry, fault rupture mechanisms, maximum earthquake magnitudes, and earthquake recurrence models. In this assessment, we characterize six shallow crustal fault sources, nine shallow crustal uniform-area sources, one subduction interface source, and one subduction in-slab source (Figure 2). For areal seismic sources, lower seismogenic depths between 20 km and 40 km were adopted following [11] and [12]. Lower seismogenic depths between 15 km to 35 km were adopted for shallow crustal fault sources following [11]. The minimum magnitude used for hazard calculations is Mw 5 because it is the smallest single earthquake with ground motions expected to result in damage to modern, well-engineered structures.

Shallow Crustal Sources

Faults

We defined six crustal faults for the seismic source model based on [11] and our analyses: Owen Stanley 1 (OST-1), Owen Stanley 2 (OST-2), Owen Stanley 3 (OST-3), Owen Stanley 4 (OST-4), Owen Stanley 5 (OST-5), and Southern Highlands Thrust (SHT). We revised Owen Stanley fault parameters used by [11] based on more current information on the Owen Stanley fault structure and geological history. The key changes were:

- Segmentation of the Owen Stanley fault based on improved understanding of the along-strike fault slip sense (e.g., [13]).
- Refined fault slip rate estimates based on investigations reported by [2] for OST-1, OST-2, OST-3, and OST-5, and by [14] for OST-4.
- Modified locations for the trace of OST-2, OST-3, and OST-4 fault sections from the GEM Active Faults Database [15] to align fault trace location with topography on Papuan Peninsula.

We computed earthquake occurrence rates using a revised maximum magnitude (Mmax) based on fault areas and the magnitude-area scaling relationship of [16], revised average fault slip rates, and an assumed *b-value* of 0.7. Table 1 lists the parameters used for the crustal fault sources.

Table 1. Mapped Crustal Fault Sources and Source Model Parameters within ~450 km of Port Moresby.

Fault	Closest Distance to Site (km)	Dip (°)[(1)]	Fault Type[(2)]	Estimated Average Slip Rate (mm/yr.)[(3)]	Seismogenic Depth (km)[(1)]	Maximum Earthquake Magnitude (Mw)[(4)]	Assumed Magnitude-Frequency Distribution[(5)]
OST-1	243	45	R	10	24	7.4	G-R
OST-2	91	45	R	5	24	7.8	G-R
OST-3	93	60	SS	3	24	7.7	G-R
OST-4	192	30	N	10	15	7.9	G-R
OST-5	414	60	SS	10	15	7.0	G-R
SHT	317	30	R	10	35	8.4	G-R

Notes

1. Estimates from [11]
2. R: Reverse Fault; SS: Strike-slip Fault; N: Normal Fault. From [13]
3. Slip rate estimates from [2] and [14]
4. Based on the magnitude-area scaling relationship of [16]
5. G-R: [17]

Distributed Sources

Figure 2 shows the uniform-area sources of the seismic source model developed for this assessment. These area sources are those from [18] and [12], but further refined with more recent information and with a focus on sources that could impact Port Moresby. Earthquake occurrence parameters were computed using the seismicity catalog compiled for this assessment for all uniform-area sources, except for PNG2. Earthquake recurrence parameters from [16] were adopted for PNG2 as there were insufficient earthquakes in the project catalog to yield robust activity rate estimates. In some cases, other parameters were redefined based on our judgement. Seismic source zones farther than 500 km from the site are assumed to contribute a negligible seismic hazard and were, therefore, excluded from the hazard calculations.

Subduction Zone Sources

Plate Interface fault

The New Britain subduction zone lies approximately 260 km from Port Moresby (Figure 1) and is the contact between the subducting Solomon Sea microplate and the overriding Pacific Plate. The eastern end of the New Britain subduction interface is east of New Ireland, where it continues to the east as the South Solomon subduction interface. The subduction interface to the west transitions to the Ramu-Markham fault, a likely inactive trench because recent continent-island arc collision likely ended active subduction. An Mw 7.8 earthquake in November 2000 on the New Britain plate interface fault was considered by [19] to have been triggered by an Mw 8.0 transform fault earthquake three hours earlier at the North and South Bismarck microplate boundary.

We used Slab 2.0 [20] to model the New Britain subduction interface source as a fault plane dipping from 0 to 50 km depth. The coseismic fault rupture area governs the earthquake magnitude, the length of individual fault ruptures along the New Britain subduction interface and the depth. For the New Britain subduction interface with a total plate velocity of 90 mm/yr. [22], we applied a coupling coefficient of 0.24 (i.e., 24% of the slip is seismogenic with 76% of plate motion not generating major earthquakes; [21]). The effective slip rate (i.e., the amount accommodated seismically) is 21.6 mm/yr calculated as the product of the slip rate and the coupling coefficient (i.e., 90*0.24 = 21.6 mm/yr.). Although there is uncertainty in the upper and lower seismogenic depths, effective slip, and coupling coefficient for the New Britain subduction interface, we used only preferred values because the large source-to-site distance results in a low contribution to the total hazard at Port Moresby.

In-slab sources

We modelled the New Britain in-slab source as a dipping seismic source at the top of the subducting slab between 50 km and 200 km depth. Recurrence parameters for the New Britain in-slab source were calculated by selecting a subset of the project catalog from between the top and bottom edge coordinates of the defined fault plane and below 50 km depth. This approach collapses the seismicity occurring on multiple surfaces onto a single surface within the slab. The impact on the total hazard at Port Moresby, however, is low.

The selection of the maximum moment magnitude, Mmax, for in-slab sources is difficult because of the deep and largely obscured subducted plate. For this assessment, we estimated the Mmax from review of global historical magnitudes within in-slab sources. To account for the uncertainty in the Mmax for the New Britain in-slab source, we incorporated a weighted range for Mmax from Mw 8.0 (lower), Mw 8.2 (preferred), Mw 8.4 (upper), and weighted 0.2, 0.6, 0.2, respectively.

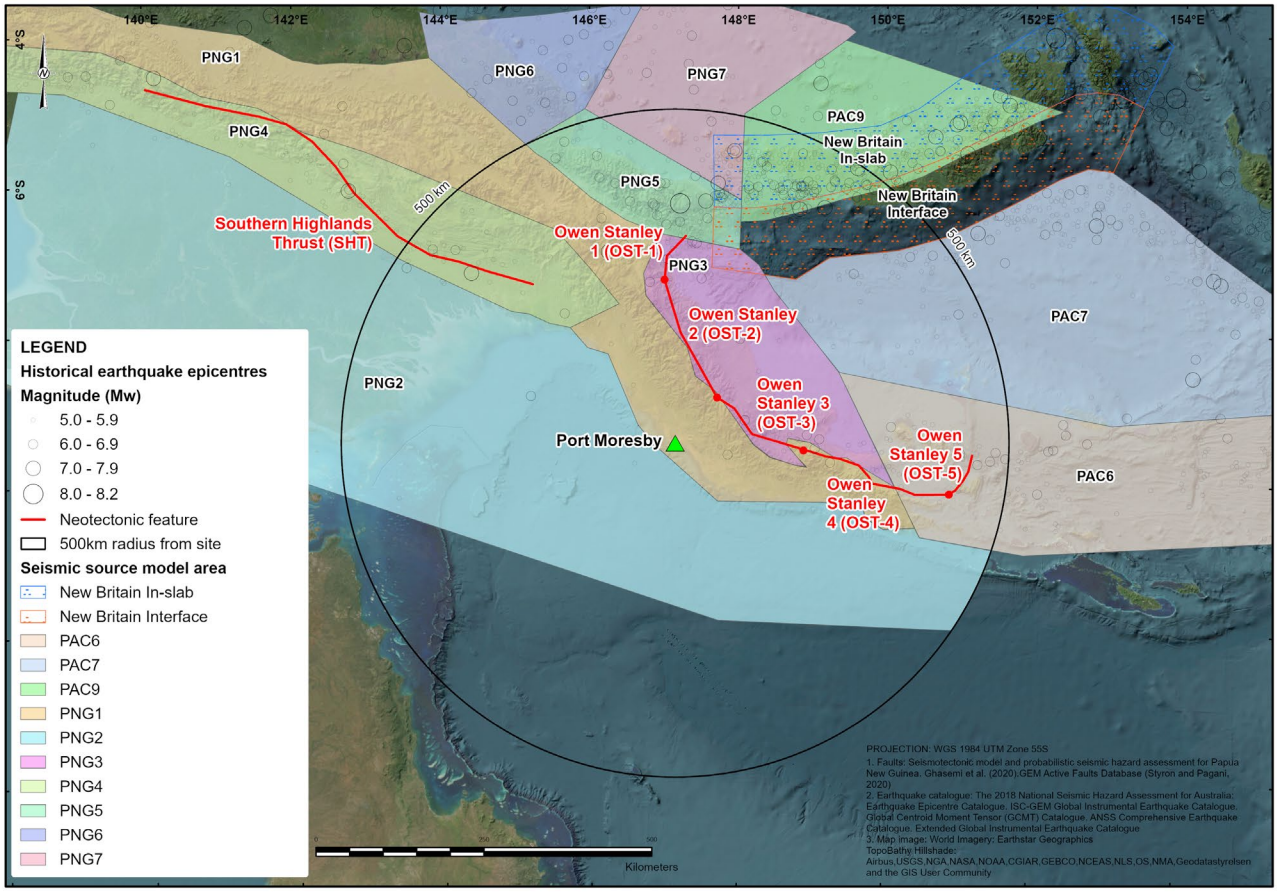

Figure 2: Seismic source model for Port Moresby. Crustal uniform-area sources area shown as solid polygons and subduction sources are shown as stippled polygons.

GROUND MOTION MODELS

Seismic hazard analysis uses ground motion models (GMM) to estimate the source-to-site attenuation of earthquake ground motions at PGA and at other spectral periods. GMMs are empirically based, with the calculated accelerations typically assuming 5% of critical damping, as in this assessment. The GMMs were selected based on the similarity between the tectonic and geologic conditions of the region and those where the earthquake motions were recorded and used to derive the empirical GMMs. The GMMs and their weights, including additional epistemic uncertainty, are described below.

Shallow Crustal

The Pacific Earthquake Engineering Research Center (PEER) Next Generation of Ground Motion Attenuation Phase 2 Project (NGA-West2 Project) GMMs were used in this study for earthquake ground motion calculations for all crustal seismic sources. The NGA-West2 GMMs were developed through a systematic process using improved strong ground motion recordings from tectonic plate boundaries, primarily from the western United States, Turkey, Japan, New Zealand, and other seismically active regions around the world. Spectral accelerations are estimated as a function of earthquake magnitude, source-to-site distance, fault geometry, and time-averaged shear-wave velocity in the upper 30 m below the site ground or reference surface (i.e., V_{S30}).

Subduction Zone

Subduction earthquake sources include both the subduction interface and subduction in-slab sources. GMMs have been developed for each of the interface and in-slab sources independently. Four GMMs for subduction zone earthquakes— [23], [24], [25], and [26] were evaluated for use in this assessment. These GMMs were developed as a part of the Next-Generation Attenuation for subduction zone regions project (NGA-Sub) completed in 2020. Three of the four available NGA-Sub GMMs were adopted with global coefficients for the interface and in-slab sources. We have no basis to distinguish if one of the GMMs provides a better representation of the source-to-site attenuation for subduction earthquakes in the New Britain Trench. The

[26] GMM was developed specifically for Japanese subduction zones using only Japanese strong motion data and is not yet used widely outside of Japan.

Figure 3 is the summary logic tree showing the sources, weights used for maximum earthquake magnitudes, and the weights for GMMs as applied in this assessment. Uncertainties in the earthquake recurrence parameters and maximum magnitude estimates were incorporated by applying weighted earthquake occurrence rates. This approach has the benefit of significantly improving computational efficiency within the OpenQuake software engine. These uncertainties, however, are incomplete for a fractile analysis, and fractiles represent only minimum estimates of uncertainty.

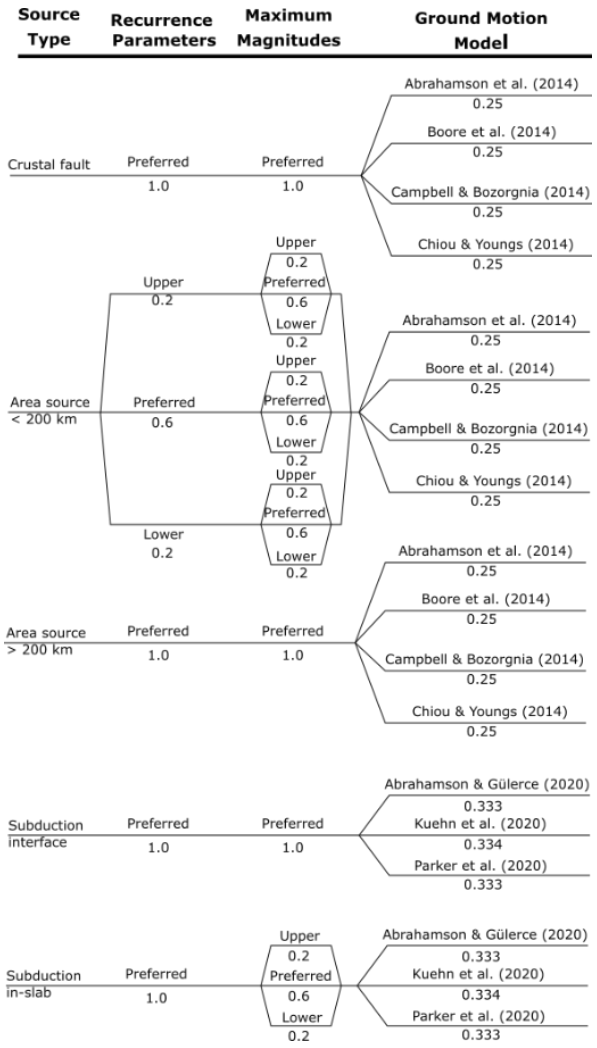

Figure 3: Logic tree for the Seismic Sources.

HAZARD RESULTS

The seismic hazard analysis was completed for a site in downtown Port Moresby with an assumed V_{S30} of 760 m/s. Calculations were made using the OpenQuake Software Engine (v.3.11.3) developed by the Global Earthquake Model Foundation (www.globalquakemodel.org). We applied a V_{S30} of 760 m/s because it is a typical ground conditions applied in modern building codes such as ASCE 7-16, 7-22, NBCC 2020, and Eurocode 8.

Hazard Curves

Hazard curves describe mean earthquake acceleration values at different AEPs at a given spectral period. Figure 4 shows mean hazard curves for selected spectral periods. The 1/43, 1/475, and 1/2,475 AEPs are also shown. The mean hazard curves are the result of summing weighted hazard curves as developed from each branch of the logic tree (Figure 3).

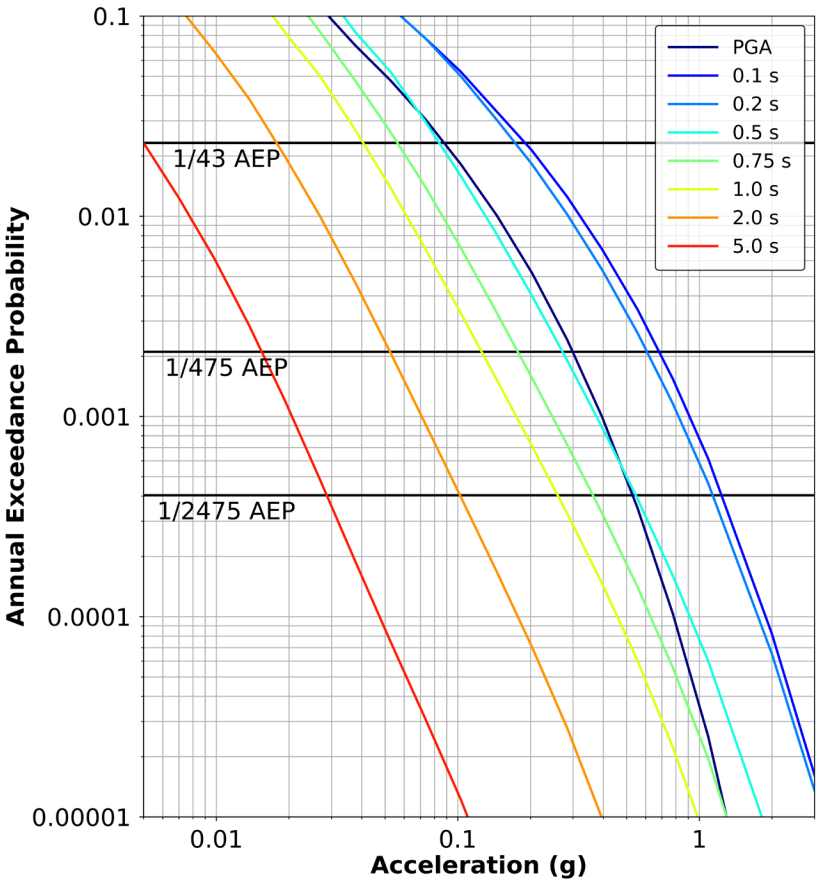

Figure 4: Mean Hazard Curves for Selected Spectral Periods.

Uniform Hazard Response Spectra

Figure 5 shows the mean uniform hazard acceleration response spectra (5%-damped) (UHRS) along with the 16th, 50th (median), and 84th fractiles for a 1/475 AEP and 1/2,475 AEP. The fractiles illustrate the minimum uncertainty associated with the mean value. Table 2 lists the mean spectral ordinates for the UHRS at 1/475 and 1/2475 AEPs.

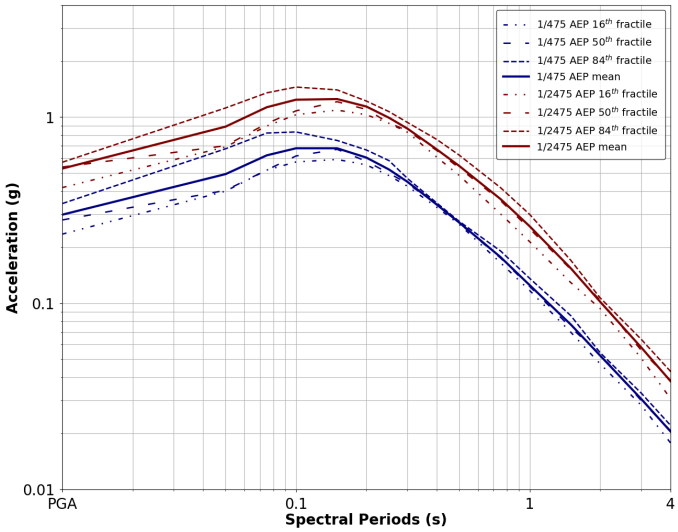

Figure 5: Uniform hazard response spectra for the mean and selected fractiles at 1/475 AEP and 1/2,475 AEP.

Table 2. Mean Uniform Hazard Response Spectral Ordinates for 1/475 and 1/2,475 AEPs.

Spectral Period (s)	Mean Acceleration (1/475 AEP) (g)	Mean Acceleration (1/2,475 AEP) (g)
PGA	0.299	0.529
0.1	0.680	1.235
0.2	0.606	1.136
0.3	0.449	0.867
0.5	0.271	0.546
1.0	0.125	0.259
2.0	0.052	0.102
3.0	0.031	0.058
5.0	0.015	0.029
10.0	0.007	0.014

Magnitude-Distance Deaggregation

Magnitude-distance deaggregation allows identification of the major earthquake sources that contribute to the total mean hazard at a specified spectral period and AEP. In this assessment, deaggregation was completed for 0.25 magnitude and 20 km bins. Epsilon is a parameter of ground-motion uncertainty that further improves the diagnostic capability of magnitude-distance hazard deaggregation. The magnitude-distance deaggregation is color-coded by epsilon in one-sigma bins.

Figure 6 shows the magnitude-distance deaggregation results of the mean UHRS at PGA, 0.2 s, 1.0 s, and 5.0 s for 1/475 AEP. Figure 7 shows the magnitude-distance deaggregation results of the mean UHRS at PGA, 0.2 s, 1.0 s, and 5.0 s for 1/2,475 AEP. The deaggregation of the hazard results for the Port Moresby site indicate that the PGA hazard at a 1/475 AEP is dominated by shallow crustal earthquakes of <Mw 6.5 within about 40 to 60 km of Port Moresby. At lesser AEPs, the contribution from shallow crustal earthquakes increases with larger magnitudes (Mw 6.0 to Mw 8.0) at greater distances. The contribution of the New Britain subduction zone at about 270 km from Port Moresby, and shallow crustal faults (Owen Stanley Fault Zone ~100 km distance) shows only at spectral periods >1 s and lower AEPs.

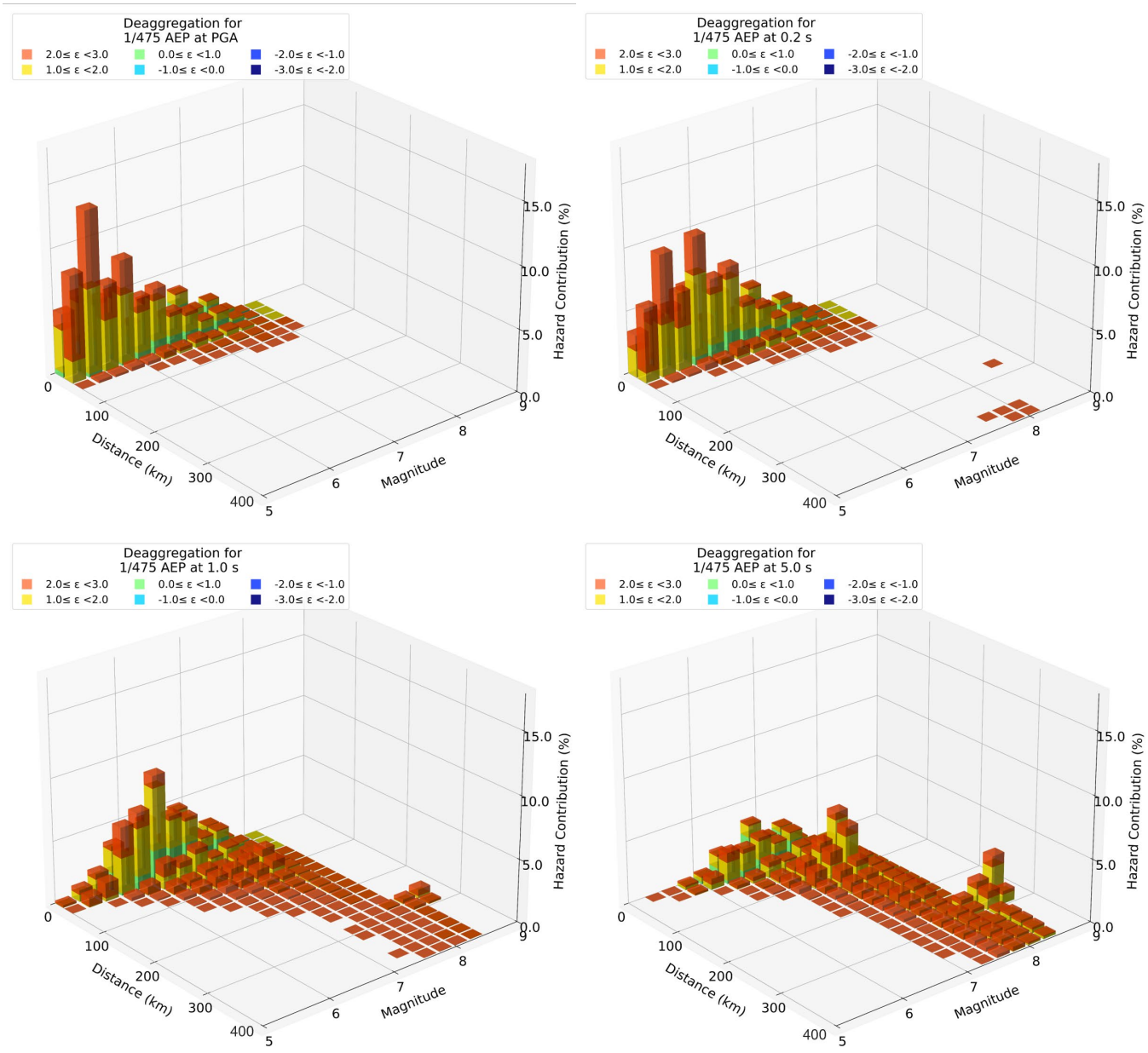

Figure 6: Magnitude-distance-epsilon deaggregation at 1/475 AEP for selected spectral periods.

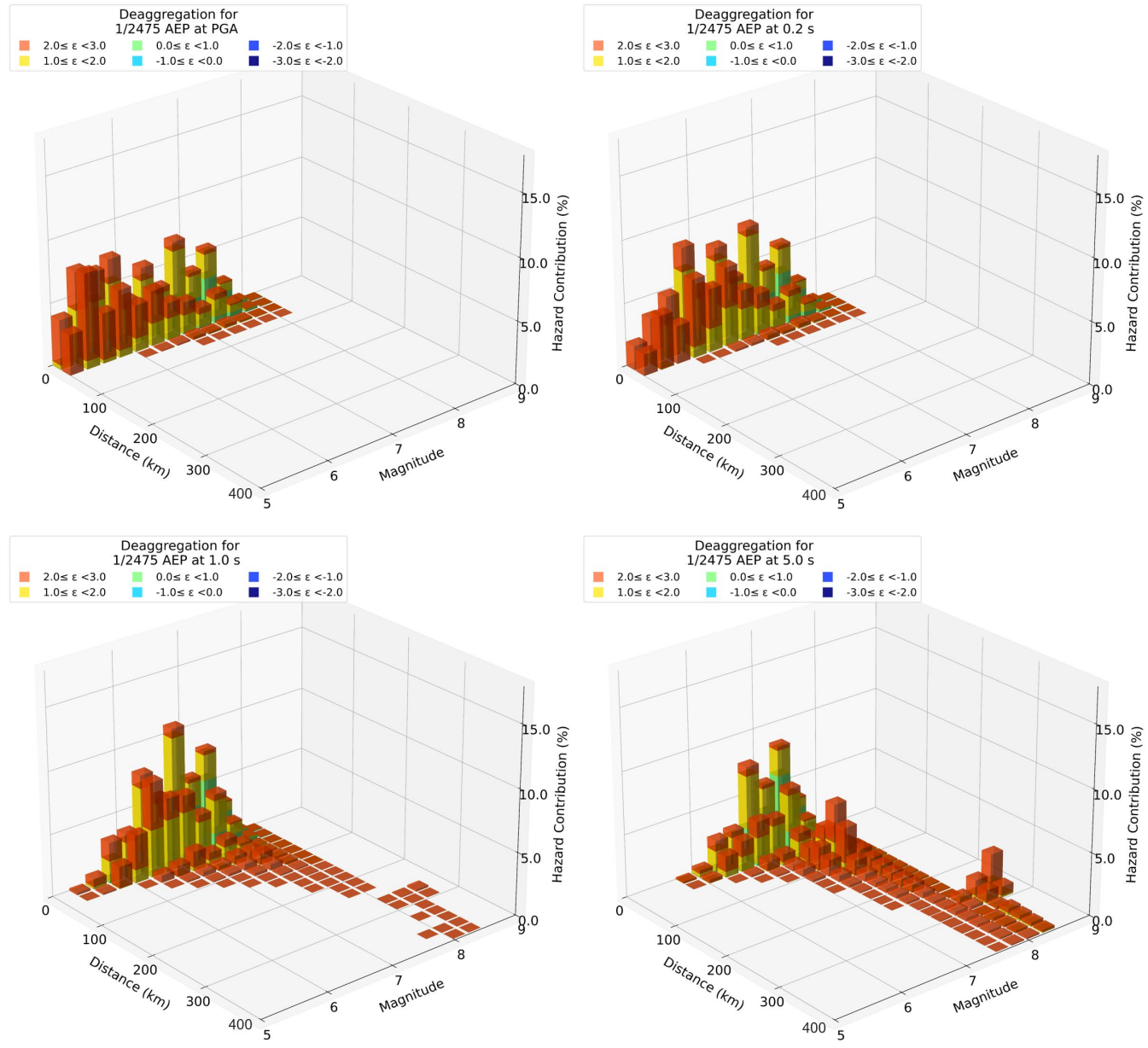

Figure 7: Magnitude-distance-epsilon deaggregation at 1/475 AEP for selected spectral periods.

COMPARISONS TO EXISTING HAZARD ESTIMATES

We used the seismic source files developed by [3] and [11] in OpenQuake v3.11.4 and applied the same GMMs as [3] and [11] for spectral accelerations (5%-damped) at AEPs of 1/475 and 1/2475. This procedure permitted direct comparison (i.e., not based on contour interpolation) between the 2019 NSHM [11] and our results. This assessment estimates greater spectral accelerations with the greatest differences (~100%) at PGA. Differences decrease with increasing spectral period to be similar at periods longer than about 2 s. We consider the spectral acceleration differences result from the different technical approaches of [3] and [11] and in this assessment. We discuss the differences further below.

Selected Ground Motion Models: For crustal sources, we applied four NGA-West2 ergodic global models with equal weight. One NGA-West2 GMM and two other GMMs, all equally weighted, were applied by [3] and [11]. We also applied the recent (2020) NGA-Sub GMMs for subduction interface and in-slab earthquake sources while [3] and [11] used older, pre-NGA-Sub GMMs. Differences in the selection and weighting of GMMs often result in spectral acceleration differences for the same

earthquake magnitude and distance, particularly at shorter periods (i.e., PGA to ~0.3 s) because the GMMs control the overall response spectral shape.

Gridded-Area Sources: In contrast to the 2016 NSHM for Papua New Guinea [18] and this assessment, [11] modelled crustal earthquake sources less than Mw 6.5 with a 0.1° by 0.1° (~11 km by 11 km) grid of earthquake activity rates and *b-values* based on Gaussian smoothing of their declustered earthquake catalog. Gridded-area sources preserve the historical earthquake pattern to represent the expected future distribution of earthquakes. By contrast, the uniform-area source model approach used by [18] and in this assessment assumes a uniform rate of earthquakes across areas with similar tectonic structure and history. The 2019 NSHM for Papua New Guinea has the larger earthquakes only on the mapped faults. For low AEPs, the uniform-area sources model the longer-term distribution of earthquakes better because larger earthquakes (i.e., Mw >6.5) can occur away from mapped faults.

Fault Sources: The source model for the Owen Stanley fault was refined from [18] and [3] by segmenting it based on recent models of fault geometry and average slip-rate studies (see discussion above). We consider that the location and rate of activity of the major seismogenic faults in Papua New Guinea are poorly constrained, particularly given the remoteness and thick vegetation cover in much of Papua New Guinea. The source models proposed by [3] and [11] do not appear to account for Mw >6.5 earthquakes away from the mapped faults. The uniform-area seismic source model appears more appropriate than a gridded-area model given this substantial lack of information.

The difference between the results obtained in this assessment and [11] demonstrates that the seismic hazard at Port Moresby is sensitive to the approach used to model the seismic sources, particularly the use of uniform-area rather than gridded-area background source zones for background earthquakes. In this assessment, the decision to allow large magnitude ruptures (Mw >6.5) away from the mapped faults reflects the poorly constrained nature of mapped active faults in PNG near Port Moresby.

CONCLUSIONS

Stiff soils sites in Port Moresby have a mean PGA estimate of 0.30 g and 0.53 g at 1/475 and 1/2,475 AEPs, respectively. Deaggregation of the 1/475 AEP and 1/2,475 AEP hazard at periods of PGA, 0.2, 1.0, and 5 s indicates that the seismic hazard at Port Moresby is dominated by shallow crustal earthquakes (Mw 5.75 to Mw 6.5) at distances less than about 40 km for periods less than 1.0 s. Mw 7+ earthquakes at distances at about 100 km dominate the hazard at periods longer than 1.0 s. The hazard contribution from the New Britain subduction zone and the Owen Stanley fault to the north is evident only at longer spectral periods (>1 s) and lower AEPs. The differences between the site-specific results presented here and previous regional source models (e.g., [11]) demonstrate that the seismic hazard in Port Moresby is sensitive to the approach used to characterize the seismic sources, especially the treatment of distributed background seismic sources.

ACKNOWLEDGMENTS

The authors acknowledge their use of the OpenQuake software (v3.11.4), developed by the Global Earthquake Model Foundation. We are grateful for inputs and support provided by our WSP colleagues in USA and New Zealand.

REFERENCES

[1] Baldwin, S. L., Fitzgerald, P. G., & Webb, L. E. (2012). Tectonics of the New Guinea Region. *Annual Review of Earth and Planetary Sciences,* 40(1), 495–520. https://doi.org/10.1146/annurev-earth-040809-152540.

[2] Koulali, A., Tregoning, P., McClusky, S., Stanaway, R., Wallace, L., & Lister, G. (2015). New Insights into the present-day kinematics of the central and western Papua New Guinea from GPS. *Geophysical Journal International,* 202(2), 993–1004. https://doi.org/10.1093/gji/ggv2000

[3] Ghasemi, H., Cummins, P., Weatherill, G., McKee, C., Hazelwood, M., & Allen, T. (2020a). *National Probabilistic Seismic Hazard Assessment for Papua New Guinea: 2019 Revision*. Geoscience Australia Record 2020.029. https://doi.org/10.11636

[4] Allen, T. I., Leonard, M., Ghasemi, H., & Gibson, G. (2018). *The 2018 National Seismic Hazard Assessment for Australia – earthquake epicentre catalogue.* Geoscience Australia, Record 2018.030. https://doi.org/10.11636

[5] Styron, R., & Pagani, M. (2020). The GEM Global Active Faults Database. *Earthquake Spectra, 36*(1_suppl), 160–180. https://doi.org/10.1177/8755293020944182

[6] Ekström, G., Nettles, M., & Dziewoński, A. M. (2012). The global CMT project 2004-2010: Centroid-moment tensors for 13,017 earthquakes. *Physics of the Earth and Planetary Interiors*, 200–201, 1–9. https://doi.org/10.1016/j.pepi.2012.04.002

[7] United States Geological Survey (USGS). (2020). *ANSS-Advanced National Seismic System*. USGS Information Sheet. ANSS - Advanced National Seismic System | U.S. Geological Survey (usgs.gov).

[8] Weatherill, G. A., Pagani, M., & Garcia, J. (2016). Exploring earthquake databases for the creation of magnitude-homogeneous catalogues: Tools for application on a regional and global scale. *Geophysical Journal International*, 206(3), 1652–1676. https://doi.org/10.1093/gji/ggw232

[9] Gardner, J. K., & Knopoff, L. (1974). Is the sequence of earthquakes in Southern California, with aftershocks removed, Poissonian? *Bulletin of the Seismological Society of America*, 64(5). https://doi.org/1363-1367/10.1785/BSSA0640051363

[10] Stepp, J. C., (1972). Analysis of Completeness of the Earthquake Sample in the Puget Sound Area and Its Effect on Statistical Estimates of Earthquake Hazard, in *Microzonation Conference, Proceedings of the International Conference on Microzonation for Safer Construction Research and Application*, National Science Foundation, Seattle, 897–909.

[11] Ghasemi, H., Cummins, P., Weatherill, G., McKee, C., Hazelwood, M., & Allen, T. (2020b). Seismotectonic model and probabilistic seismic hazard assessment for Papua New Guinea. *Bulletin of Earthquake Engineering*, 18(15), 6571–6605. https://doi.org/10.1007/s10518-020-00966-1

[12] Johnson, K. L., Pagani, M., & Styron, R. H. (2021). PSHA of the southern Pacific Islands. *Geophysical Journal International*, 224(3), 2149–2172. https://doi.org/10.1093/gji/ggaa530

[13] Sun, L., & Mann, P. (2021). Along-Strike Rapid Structural and Geomorphic Transition from Transpression to Strike-Slip to Transtension related to Active Microplate Rotation, Papua New Guinea. *Frontiers in Earth Science*, 9. https://www.frontiersin.org/article/10.3389/feart.2021.652352

[14] Little, T. A., Webber, S. M., Mizera, M., Boulton, C., Oesterle, J., Ellis, S., Boles, A., van der Pluijm, B., Norton, K., Seward, D., Biemiller, J. & Wallace, L. (2019). Evolution of rapidly slipping, active low-angle normal fault, Suckling-Dayman metamorphic core complex, SE Papua New Guinea. *Geological Society of America Bulletin*, 131(7-8), 1333-1363. https://doi.org/10.1130/B35051.1

[15] Styron, R., & Pagani, M. (2020). The GEM Global Active Faults Database. *Earthquake Spectra, 36*(1_suppl), 160–180. https://doi.org/10.1177/8755293020944182

[16] Wells, D. L., & Coppersmith, K. J. (1994). New empirical relationships among magnitude, rupture length, rupture width, rupture area, and surface displacement. *Bulletin of the Seismological Society of America*, 84(4), 974–1002. https://doi.org/10.1785/BSSA0840040974

[17] Gutenberg, B. & Richter, C. F. (1944). Frequency of earthquakes in California. *Bulletin of the Seismological Society of America*, 34(4), 185-188. https://doi.org/10.1785/BSSA0340040185

[18] Ghasemi, H., McKee, C., Leonard, M., Cummins, P., Moihoi, M., Spiro, S., Taranu, F., & Buri, E. (2016). Probabilistic seismic hazard map of Papua New Guinea. *Natural Hazards*, 81(2), 1003–1025. https://doi.org/10.1007/s11069-015-2117-8

[19] Hayes, G. P., Meyers, E. K., Dewey, J. W., Briggs, R. W., Earle, P. S., Benz, H. M., Smoczyk, G. M., Flamme, H. E., Barnhart, W. D., Gold, R. D., & Furlong, K. P. (2017). *Tectonic summaries of magnitude 7 and greater earthquakes from 2000 to 2015. In Tectonic summaries of magnitude 7 and greater earthquakes from 2000 to 2015*, USGS Open-File Report 2016–1192. U.S. Geological Survey. https://doi.org/10.3133/ofr20161192

[20] Hayes, G. P., Moore, G. L., Portner, D. E., Hearne, M., Flamme, H., Furtney, M., & Smoczyk, G. M. (2018). Slab2, a comprehensive subduction zone geometry model. *Science*, 362(6410), 58–61. https://doi.org/10.1126/science.aat4723

[21] Heuret, A., Lallemand, S., Funiciello, F., Piromallo, C., & Faccenna, C. (2011). Physical characteristics of subduction interface type seismogenic zones revisited. *Geochemistry, Geophysics, Geosystems*, 12(1). https://doi.org/10.1029/2010GC003230

[22] Bird, P. (2003). An updated digital model of plate boundaries. *Geochemistry, Geophysics, Geosystems*, 4(3). https://doi.org/10.1029/2001GC000252

[23] Abrahamson, N., and Gülerce, Z. (2020). *Regionalized Ground-Motion Models for Subduction Earthquakes Based on the NGA-SUB Database*. Pacific Earthquake Engineering Research Center (PEER) Report No. 2020-25

[24] Kuehn, N., Bozorgnia, Y., Campbell, K. W., and Gregor, N. (2020). *Partially Non-Ergodic Ground-Motion Model for Subduction Regions using the NGA-Subduction Database*. PEER Report No. 2020-04

[25] Parker, G. A., Stewart, J. P., Boore, D. M., Atkinson, G. M., and Hassani, B. (2020). NGA-subduction global ground motion models with regional adjustment factors. *Earthquake Spectra*, 38(1), 456-493. https://doi.org/10.1177/87552930211034889

[26] Si, H., Midorikawa, S., and Kishida, T. (2020). *Development of NGA-Sub Ground-Motion Model of 5%-Damped Pseudo-Spectral Acceleration Based on Database for Subduction Earthquakes in Japan*. PEER Report 2020-06.